Monte Carlo study of efficiency roll-off of phosphorescent organic light-emitting diodes : Evidence for dominant role of triplet-polaron quenching.

AIP | Applied Physics Letters

Monte Carlo study of efficiency roll-off of phosphorescent organic light-emitting diodes: Evidence for dominant role of triplet-polaron quenching

H. van Eersel, P. A. Bobbert, R. A. J. Janssen, and R. Coehoorn

Citation: Applied Physics Letters **105**, 143303 (2014); doi: 10.1063/1.4897534
View online: http://dx.doi.org/10.1063/1.4897534
View Table of Contents: http://scitation.aip.org/content/aip/journal/apl/105/14?ver=pdfcov
Published by the AIP Publishing

Monte Carlo study of efficiency roll-off of phosphorescent organic light-emitting diodes: Evidence for dominant role of triplet-polaron quenching

H. van Eersel,[1,2,a)] P. A. Bobbert,[1] R. A. J. Janssen,[1] and R. Coehoorn[1,2]
[1]*Department of Applied Physics, Eindhoven University of Technology, P.O. Box 513, 5600 MB Eindhoven, The Netherlands*
[2]*Philips Research Laboratories, High Tech Campus 4, 5656 AE Eindhoven, The Netherlands*

(Received 24 July 2014; accepted 26 September 2014; published online 9 October 2014)

We present an advanced molecular-scale organic light-emitting diode (OLED) model, integrating both electronic and excitonic processes. Using this model, we can reproduce the measured efficiency roll-off for prototypical phosphorescent OLED stacks based on the green dye tris[2-phenylpyridine]iridium ($Ir(ppy)_3$) and the red dye octaethylporphine platinum (PtOEP) and study the cause of the roll-off as function of the current density. Both the voltage *versus* current density characteristics and roll-off agree well with experimental data. Surprisingly, the results of the simulations lead us to conclude that, contrary to what is often assumed, not triplet-triplet annihilation but triplet-polaron quenching is the dominant mechanism causing the roll-off under realistic operating conditions. Simulations for devices with an optimized recombination profile, achieved by carefully tuning the dye trap depth, show that it will be possible to fabricate OLEDs with a drastically reduced roll-off. It is envisaged that J_{90}, the current density at which the efficiency is reduced to 90%, can be increased by almost one order of magnitude as compared to the experimental state-of-the-art. © *2014 AIP Publishing LLC*. [http://dx.doi.org/10.1063/1.4897534]

Excitonic processes play a key role in organic optoelectronic devices. The ultimately attainable internal quantum efficiency (IQE) in, e.g., organic light-emitting diodes (OLEDs), organic photovoltaic devices, and light-emitting field-effect transistors is determined by the complex interplay of exciton radiative and non-radiative decay, diffusion, and dissociation. At high excitation densities, additional quenching can occur due to exciton-exciton and exciton-charge interactions. These bimolecular processes present a considerable challenge to the development of electrically pumped organic lasers,[1] and cause in phosphorescent OLEDs a decrease of the IQE with increasing current density.[2,3] Elucidating the origin of this *roll-off* and disentangling the roles of both types of loss processes has been a subject of intensive study.[2–7] However, so far, no widely accepted picture has emerged. Obtaining such a picture is hampered by the need to carefully consider the strong spatial non-uniformity of the charge and exciton densities in actual devices.

In this letter, we focus on phosphorescent OLEDs, and demonstrate, using experimentally determined parameters, how advanced molecular-scale simulations including all charge transport and excitonic processes can reproduce experimental roll-off curves. Furthermore, we show how the simulations can be employed to analyze the cause of the efficiency roll-off. In addition to possible loss processes related to non-ideal confinement of charge carriers and excitons to the thin emissive layer (EML) which contains the dye molecules, the simulations also include the effects of triplet-polaron quenching (TPQ) and triplet-triplet annihilation (TTA) on the efficiency roll-off. TPQ occurs upon the creation of an excited polaron state after close encounter with an exciton, after which the excess energy is lost by thermalization, whereas TTA is caused by the fusion of two triplet excitons to a high-energy excitonic state, followed again by a loss of the excess energy by thermalization, so that effectively one triplet exciton is lost. TTA[2] as well as TPQ[5,7] have been argued to be the predominant cause of the roll-off. The experimental evidence to support either of these points of view has been based on time-dependent photoluminescence,[4] and steady state[2] and time-dependent[7] electroluminescence measurements. The simulations allow us to study the interplay between both competing effects, and reveal that in archetypal OLEDs at low voltages TPQ is the predominant cause of the roll-off.

We use a kinetic Monte Carlo (MC) OLED device model within which charge transport and excitonic processes are included in an integral manner. The model is based on hopping on a three-dimensional grid of sites on a simple cubic lattice, representing the molecules. Charge carrier injection, transport, and exciton generation are treated as described in Ref. 8; Coulomb interactions and image charge effects are included. The extended model also includes exciton diffusion by both the Förster[9] and Dexter[10] mechanisms, radiative and non-radiative decay, exciton dissociation, and losses due to TPQ and TTA, as described further below. The model is mechanistic, i.e., based entirely on a physical description of the processes included and using measurable parameters, so that no fitting is required. MC simulations have been used before in studies of charge transport[11] and exciton transfer[12] in disordered organic materials. However, the charge transport and excitonic models have never been integrated in a full multilayer device model.

We investigate the shape of the roll-off for two prototypical OLED stacks, studied intensively in the literature,[2,6,13]

a)h.v.eersel@tue.nl

based on the green phosphorescent emitter tris[2-phenylpyridine]iridium ($Ir(ppy)_3$) and the red phosphorescent emitter octaethylporphine platinum (PtOEP). As the triplet radiative lifetime of $Ir(ppy)_3$ is much shorter than that of PtOEP ($\sim 1\,\mu s$ *vs* $\sim 100\,\mu s$), a comparison between both devices will reveal to what extent the relative contributions of TPQ and TTA to the roll-off are sensitive to the emissive lifetime. The layer structures are shown in Fig. 1(a). Both dyes are embedded in a matrix consisting of 4,4′-bis[9-carbazolyl]-2,2′-biphenyl (CBP). This emissive layer is sandwiched between other layers that facilitate electron and hole injection, transport, and blocking. The electrodes consist of indium tin oxide (ITO) and lithium fluoride/aluminum (LiF/Al). The simulation results are compared to the experimental data presented by Giebink and Forrest.[6]

The simulation parameters used were chosen as follows. The highest occupied molecular orbital (HOMO) energies were obtained from ultraviolet photoemission spectroscopy (UPS),[14–16] and the lowest unoccupied molecular orbital (LUMO) was obtained by adding the measured optical gap. The values are given in Fig. 1(a). This neglects the exciton binding energy; if taken equal for all materials, the resulting underestimation of the LUMO would result in a horizontal shift of the $J(V)$ curve. We note that we do take the exciton binding energy into account (1.0 eV for all materials) for calculating exciton generation and dissociation rates.[17] Due to a lack of detailed information on the charge transport parameters, we adopt for all materials and for both electrons and holes the same approximate approach, viz. Miller-Abrahams (MA) hopping[19–21] in a random Gaussian Density of States (DOS) with a width $\sigma = 0.1$ eV, a site density $N_t = 10^{27}\,m^{-3}$, a wavefunction decay length of $\lambda = 0.3$ nm and a hopping attempt frequency to a first nearest neighbor (at 1 nm distance) equal to $3.3 \times 10^{10}\,s^{-1}$ at 300 K. The latter value is a typical attempt frequency of holes in α-NPD.[22] The same MA formalism is employed to describe exciton generation and dissociation. Instantaneous intersystem crossing is assumed, so that only triplets are considered. The radiative (non-radiative) decay rates used are $\Gamma_{r(nr)} = 1.0$ (0.3) μs^{-1} for $Ir(ppy)_3$[23] and 0.010 (0.051) μs^{-1} for PtOEP,[24] corresponding to a photoluminescence quantum efficiency (PLQE) equal to 77% and 16%, respectively. Triplet diffusion between the dye molecules is described as a sum of long-range Förster processes with a Förster radius equal to $R_{F,diff} = 1.5$ nm, the approximate range found in Ref. 25 for various materials, and short-range Dexter processes with an $\exp(-2R/\lambda)$ distance (R) dependence and with a rate equal to the Förster rate at $R = 1.5$ nm. The same rate was assumed for the Dexter transfer between the host and guest molecules. The triplet energy levels—determining the exciton diffusion—were taken from experiment[14,18] and Gaussian excitonic energetic disorder of 0.1 eV was assumed. At least 124 possible neighbors were considered for each charge or exciton hop. More details on the simulation method and an overview of all parameters can be found in the Section S1 of the supplementary material (SM).[31]

The microscopic mechanisms of TPQ and TTA are not well established. Both Förster and Dexter mediated mechanisms have been proposed in the literature. The overall rate may be due to a multiple-step diffusion process preceding the final quenching or annihilation step occurring within a small capture radius.[3,26] We assume that for TPQ and TTA the final step occurs instantaneously upon formation of a nearest neighbor pair and neglect any direct long-range

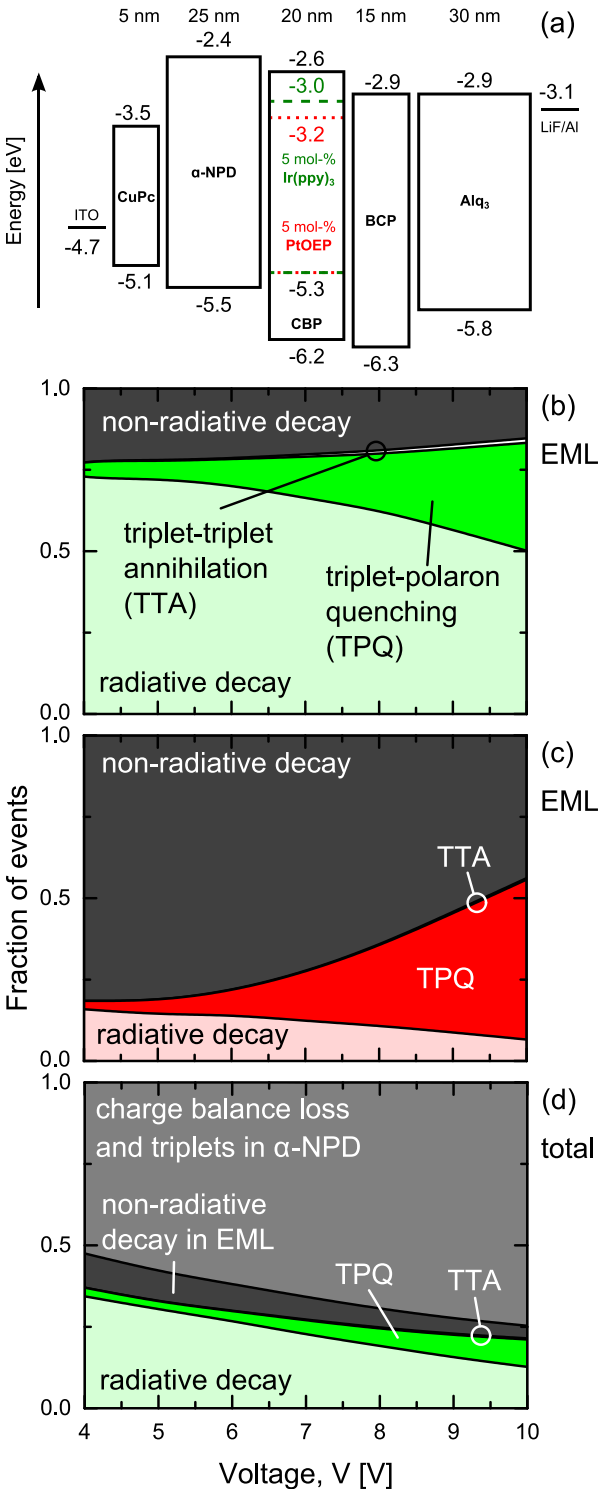

FIG. 1. (a) Energy level and layer structure of the OLEDs studied. The phosphorescent EML is sandwiched in between materials facilitating hole and electron injection, transport, and blocking: CuPc (copper phthalocyanine), α-NPD (4,4′-bis[*N*-(1-naphthyl)-*N*-phenyl-amino]biphenyl), BCP (2,9-dimethyl-4,7-diphenyl-1,10-phenanthroline) and Alq_3 (tris[8-hydroxyquinoline]aluminum); (b)–(d) Contribution of the various exciton decay processes in the EML of the $Ir(ppy)_3$ (b) and PtOEP (c) devices, and in the entire $Ir(ppy)_3$ device (d). Only a small fraction of TTA is observed: even at voltages of 6 V and above less than 2% (0.5%) for the $Ir(ppy)_3$ (PtOEP) devices.

interaction. This could be viewed as a lower bound for the actual quenching rate, in which long-range interaction most likely will also play a role. In the case of TTA, of the two triplets one randomly selected triplet remains after the annihilation.

Figure 2(a) shows that for both devices, the calculated current density *vs* voltage ($J(V)$) characteristics are reasonably close to the experimental curves, considering the assumptions made for the modeling of the charge transport. As discussed above, a shift of the LUMO levels to take the exciton binding energies properly into account would lead to a reduced current density, and hence to a reduced difference with the experimental curves. As the focus is on obtaining a general understanding of the roles of TPQ and TTA, we have chosen not to improve the agreement by further adapting the transport or energy level parameters. Instead, we discuss in Section S2 of the SM[31] the sensitivity of the simulation results to various parameter values. The results suggest that the $J(V)$ characteristics of the complete device stack are strongly determined by the charge-transport barriers due to the energy-level differences of the materials, and the dye trap depths. Varying the charge carrier mobilities of the individual materials has a comparatively small effect. Figure 2(b) shows that for $Ir(ppy)_3$ also the calculated and experimental roll-off curves agree within the error margin of the simulations. For PtOEP, the roll-off is somewhat underestimated at high current densities. This could indicate that our nearest-neighbor assumption for the quenching processes is too limited.

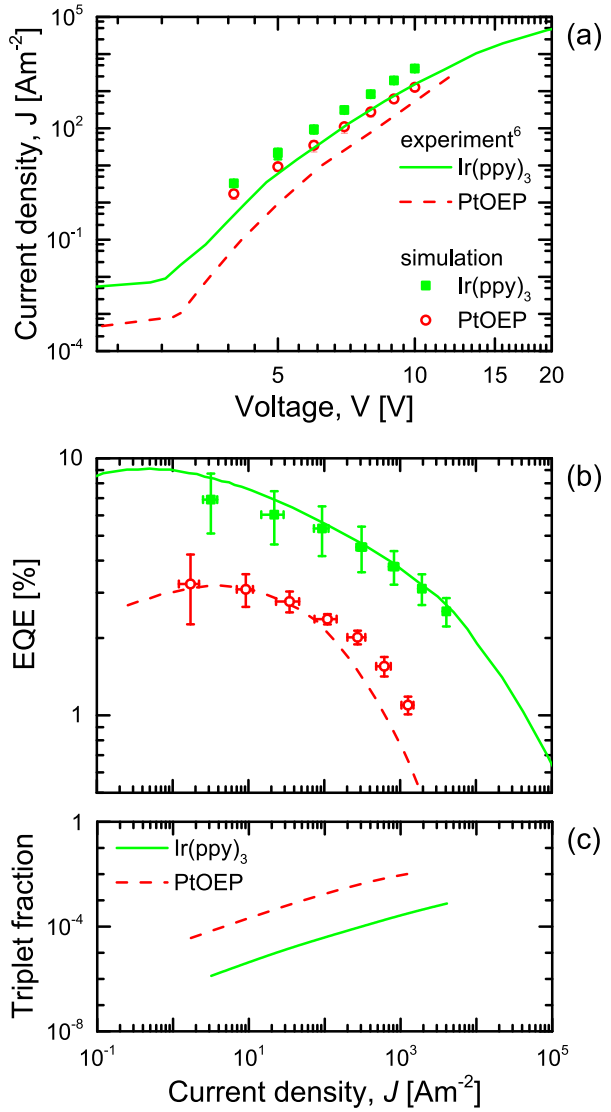

FIG. 2. (a) Simulated and experimental $J(V)$ characteristics. (b) Simulated external quantum efficiency (EQE) (assuming 20% outcoupling efficiency) and experimental EQE as a function of the current density. Experimental data from Ref. 6. (c) Fraction of EML sites occupied by triplet excitons in the simulations.

Figures 1(b) and 1(c) show the contribution of the various excitonic loss processes in the EML in both devices. At low voltages, the only significant loss process is nonradiative decay. As the voltage increases, the losses due to TPQ become significant. The losses due to TTA remain marginal. This may be understood as a result of the very small triplet diffusion lengths in the dilute systems studied, combined with a very small fraction of EML sites occupied by triplet excitons, shown in Fig. 2(c). However, for the green devices not all losses are confined to the EML: the electron blocking in the devices is found to be insufficient, leading to a reduced recombination efficiency and some emission from the α-NPD hole transporting layer (HTL). This was experimentally observed as a small blue spectral contribution by Giebink and Forrest.[6] Moreover, the triplet energy level of the α-NPD is lower than the triplet energy of $Ir(ppy)_3$, resulting in the transfer of triplets from the dye to the nonemissive electron transport layer. The contribution of these two loss mechanisms to the total efficiency of the green device is shown in Fig. 1(d). It can be seen that this not only causes the IQE at low voltages to be lower than the theoretically expected 77%, as was already suggested by Giebink and Forrest,[6] but also completely dominates the roll-off at higher voltages. For the red devices, loss of electrons to the HTL also plays a role, albeit only at higher voltages (Section S3, SM).[31] This can be understood by the lower LUMO and triplet energy of PtOEP: Blocking of electrons transported via the dye is more effective, and loss of triplets by diffusion into α-NPD does not occur.

The simulations can be employed to explore the benefits of various modifications of the layer stack to the roll-off. Figure 3(a) shows the cumulative stepwise improvement of the performance of the $Ir(ppy)_3$ devices as obtained by (1) increasing the LUMO energy of the HTL (avoiding electron loss), (2) increasing the triplet level in the HTL (avoiding exciton loss), and (3) eliminating injection barriers, symmetrizing the layer and energy level structure and reducing the guest HOMO and LUMO trap depths, Δ, to 0.3 eV (Fig. 3(b)). The beneficial effects of steps 1 and 2 have already been implemented by using thin exciton blocking layers (e.g., in Ref. 27) at the HTL/EML interface. Step 3 provides an idealized but potentially realizable OLED layer stack, with, for $\Delta = 0.2$–0.4 eV, a quite uniform recombination profile across the EML (Fig. 3(c)), a high current density at any given voltage (and hence a drastic reduction of the overvoltage), and a high value of J_{90} (the current density at which the efficiency is reduced to 90%) of 1.5×10^3 A/m^2. This value is almost one order of magnitude larger than the highest value reported to date for phosphorescent OLEDs.[3] Also for these improved devices,

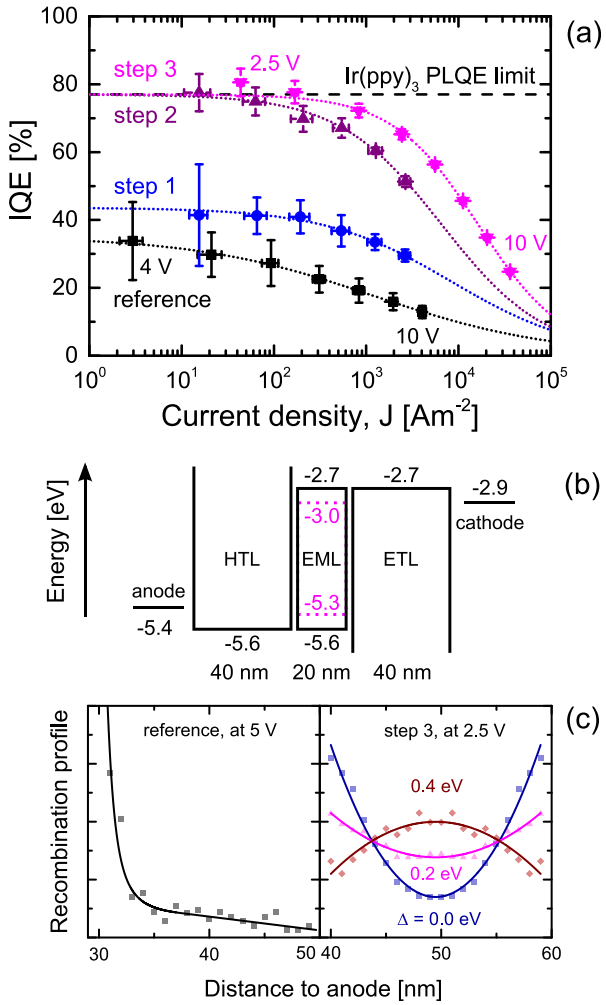

FIG. 3. (a) IQE and reduction of the roll-off after each improvement step (cumulative), compared to the reference case (black squares). (b) Energy levels in the device of step 3, with perfect electron and hole blocking. (c) Normalized recombination profile for the reference case and after step 3, for various levels of the dye trap depth Δ.

we find that the dominant contribution to the roll-off is TPQ (Section S4, SM).[31]

The result that a nonzero value of the dye trap depth is beneficial for the efficiency may seem counterintuitive at first. The effect of the dye trap depth on the efficiency of the symmetric devices is shown in Fig. 4. While the relative IQE, $\eta_{IQE}/\eta_{IQE,max}$ (closed symbols), increases significantly up to $\Delta = 0.2$ eV, there is very little effect for deeper traps. The increased trapping does, however, lead to an increase of the overvoltage. The open symbols in the figure show that the net result is a rather constant power efficiency up to $\Delta \sim 0.2$ eV, after which the efficiency decreases. This might seem to indicate that the precise value of Δ is irrelevant, if it is sufficiently small. However, around $\Delta = 0$ eV, the dissipation in the EML is a predominantly *local* and *high-energy* TPQ-dominated process, whereas around $\Delta = 0.2$ eV, the dissipation is a more *global* and *low-energy* Ohmic-loss process. Therefore, in the latter case, a significantly larger OLED lifetime is expected. An explicit study of the relationship between the roll-off and lifetime is presented in Ref. 28.

In conclusion, a fully integrated electronic-excitonic 3D Monte Carlo OLED device model has been developed. Using

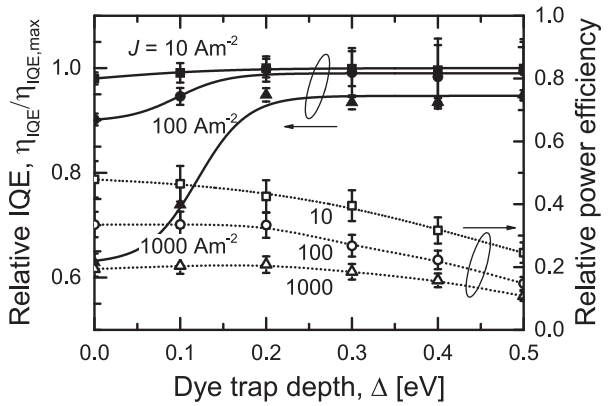

FIG. 4. The relative IQE (closed symbols) and relative power efficiency (open symbols) as function of the dye trap depth, for different current densities J. For the $J(V)$ characteristics used to calculate the power efficiency, see Section S4, SM.[31]

experimentally determined parameters, the model reproduces measured roll-off curves of intensively studied phosphorescent OLEDs with strongly different efficiencies and emissive lifetimes, based on $Ir(ppy)_3$ and PtOEP. An analysis of the excitonic processes contributing to the roll-off reveals that—under the assumption of instantaneous nearest-neighbor quenching—TPQ is the dominant process and that TTA only plays a marginal role. As a next step, we will study the effect of long-range quenching processes on the roll-off. We have also shown that by symmetrizing the stack and by using the dye as trap, we can optimize the recombination profile, thereby reducing the roll-off. This approach may lead to OLEDs in which the J_{90} value can be drastically increased beyond the values reported up till now. The excess energy released upon quenching has been linked to degradation,[29] so reducing the roll-off is also expected to improve the lifetime. The model presented in this letter can be readily applied to any arbitrary OLED layer stack, to study the molecular-scale consequences of varying the charge and excitonic interaction processes (e.g., thermally activated delayed fluorescence),[30] and the operational conditions including, e.g., the temperature and a time-dependent current density, potentially leading to further improved designs.

We would like to thank F. W. A. van Oost and J. J. M. van der Holst for laying the foundation of the Monte Carlo code, C. Weijtens for the UPS measurements, and the Philips Research e-Science department for technical support. This research was supported by the Dutch nanotechnology program NanoNextNL.

[1]Y. Setoguchi and C. Adachi, J. Appl. Phys. **108**, 064516 (2010).
[2]M. A. Baldo, C. Adachi, and S. R. Forrest, Phys. Rev. B **62**, 10967 (2000).
[3]C. Murawski, K. Leo, and M. C. Gather, Adv. Mater. **25**, 6801 (2013).
[4]S. Reineke, K. Walzer, and K. Leo, Phys. Rev. B **75**, 125328 (2007).
[5]F. X. Zang, T. C. Sum, A. C. H. Huan, T. L. Li, W. L. Li, and F. Zhu, Appl. Phys. Lett. **93**, 023309 (2008).
[6]N. C. Giebink and S. R. Forrest, Phys. Rev. B **77**, 235215 (2008).
[7]D. Song, S. Zhao, Y. Luo, and H. Aziz, Appl. Phys. Lett. **97**, 243304 (2010).
[8]M. Mesta, M. Carvelli, R. J. de Vries, H. van Eersel, J. J. M. van der Holst, M. Schober, M. Furno, B. Lüssem, K. Leo, P. Loebl, R. Coehoorn, and P. A. Bobbert, Nat. Mater. **12**, 652 (2013).
[9]T. Förster, Ann. Phys. **437**, 55 (1948).
[10]D. L. Dexter, J. Chem. Phys. **21**, 836 (1953).

[11]H. Bässler, Phys. Status Solidi B **175**, 15 (1993).
[12]G. Schönherr, R. Eiermann, H. Bässler, and M. Silver, Chem. Phys. **52**, 287 (1980).
[13]C. Adachi, R. Kwong, and S. R. Forrest, Org. Electron. **2**, 37 (2001).
[14]Measured at Philips Research Aachen.
[15]I. G. Hill, A. J. Mäkinen, and Z. H. Kafafi, Appl. Phys. Lett. **77**, 2003 (2000).
[16]C.-H. Cheng, Z.-Q. Fan, S.-K. Yu, W.-H. Jiang, X. Wang, G.-T. Du, Y.-C. Chang, and C.-Y. Ma, Appl. Phys. Lett. **88**, 213505 (2006).
[17]This value is based on the experimental singlet and triplet energies for $Ir(ppy)_3$,[18] and an estimate of the singlet exciton binding energy. See Section S1 of the supplementary material presented in Ref. 31.
[18]T. Tsuboi, H. Murayama, and A. Penzkofer, Thin Solid Films **499**, 306 (2006).
[19]A. Miller and E. Abrahams, Phys. Rev. **120**, 745 (1960).
[20]This approach avoids using the Marcus formalism, within which an additional and unknown parameter (the reorganization energy) is employed; it was found in Ref. 21 that only a small difference is expected between the mobilities as obtained within the Miller-Abrahams and Marcus formalisms.
[21]J. Cottaar, L. J. A. Koster, R. Coehoorn, and P. A. Bobbert, Phys. Rev. Lett. **107**, 136601 (2011).
[22]S. L. M. van Mensfoort, V. Shabro, R. J. de Vries, R. A. J. Janssen, and R. Coehoorn, J. Appl. Phys. **107**, 113710 (2010).
[23]S. Mladenovski, S. Reineke, and K. Neyts, Opt. Lett. **34**, 1375 (2009).
[24]A. K. Bansal, A. Penzkofer, W. Holzer, and T. Tsuboi, Mol. Cryst. Liq. Cryst. **467**, 21 (2007).
[25]Y. Kawamura, J. Brooks, J. J. Brown, H. Sasabe, and C. Adachi, Phys. Rev. Lett. **96**, 017404 (2006).
[26]Y. Zhang and S. R. Forrest, Chem. Phys. Lett. **590**, 106 (2013).
[27]T. L. Li, W. L. Li, B. Chu, Z. S. Su, Y. R. Chen, L. L. Han, D. Y. Zhang, X. Li, F. X. Zang, T. C. Sum, and A. C. H. Huan, J. Phys. D: Appl. Phys. **42**, 065103 (2009).
[28]R. Coehoorn, H. van Eersel, P. A. Bobbert, and R. A. J. Janssen, "Kinetic Monte Carlo study of the sensitivity of OLED efficiency and lifetime to materials parameters," Adv. Funct. Mater. (to be published).
[29]N. C. Giebink, B. W. D'Andrade, M. S. Weaver, P. B. Mackenzie, J. J. Brown, M. E. Thompson, and S. R. Forrest, J. Appl. Phys. **103**, 044509 (2008).
[30]H. Uoyama, K. Goushi, K. Shizu, H. Nomura, and C. Adachi, Nature **492**, 234 (2012).
[31]See supplementary material at http://dx.doi.org/10.1063/1.4897534 for information regarding details of the simulation and overview of parameters (S1), sensitivity to parameter values (S2), composition of the roll-off for the PtOEP device (S3), and $J(V)$ curves and roll-off composition in idealized OLED layer stacks (S4).